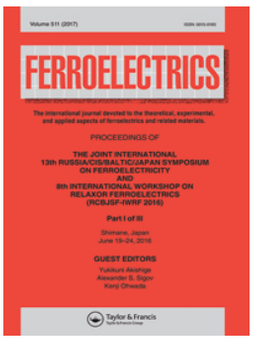

Ferroelectrics

ISSN: 0015-0193 (Print) 1563-5112 (Online) Journal homepage: http://www.tandfonline.com/loi/gfer20

Optical, electronic, and elastic properties of some $A^5B^6C^7$ ferroelectrics (A=Sb, Bi; B=S, Se; C=I, Br, Cl): First principle calculation

Husni Koc, Selami Palaz, Amirullah M. Mamedov & Ekmel Ozbay

To cite this article: Husni Koc, Selami Palaz, Amirullah M. Mamedov & Ekmel Ozbay (2017) Optical, electronic, and elastic properties of some $A^5B^6C^7$ ferroelectrics (A=Sb, Bi; B=S, Se; C=I, Br, Cl): First principle calculation, Ferroelectrics, 511:1, 22-34, DOI: 10.1080/00150193.2017.1332967

To link to this article: http://dx.doi.org/10.1080/00150193.2017.1332967

Published online: 01 Aug 2017.

FERROELECTRICS
2017, VOL. 511, 22–34
https://doi.org/10.1080/00150193.2017.1332967

Taylor & Francis
Taylor & Francis Group

Optical, electronic, and elastic properties of some $A^5B^6C^7$ ferroelectrics (A=Sb, Bi; B=S, Se; C=I, Br, Cl): First principle calculation

Husni Koc[a], Selami Palaz[b], Amirullah M. Mamedov[c,d], and Ekmel Ozbay[c]

[a]Department of Physics, Siirt University, Siirt, Turkey; [b]Department of Physics, Harran University, Sanliurfa, Turkey; [c]Nanotechnology Research Center (NANOTAM), Bilkent University, Bilkent, Ankara, Turkey; [d]International Scientific Center, Baku State University, Baku, Azerbaijan

ABSTRACT

In present paper, we focus on the structural, mechanical, electronic, and optical properties for the $A^5B^6C^7$(A = Sb, Bi; B = Te, Se; S; C = I, Br, Cl) compounds using the density functional methods in generalized gradient approximation. The lattice parameters, mechanical properties, electronic bands structures and the partial densities of states corresponding to the band structures, and optical properties are presented and analysed. Our structural estimation and some other results are in agreement with the available experimental and theoretical data.

ARTICLE HISTORY
Received 19 June 2016
Accepted 27 March 2017

KEYWORDS
Electronic properties; band structure; ferroelectrics

1. Introduction

The many $A^5B^6C^7$ (A = Sb, Bi; B = Te, Se; S; C = I, Br, Cl) compounds that are layered non-centrosymmetric materials have significant thermoelectric, photoelectric, and ferroelectric properties [1–5]. The large Rashba-type spin-orbit-coupling (SOC) in the bulk and surface electronic structure of these compounds has recently attracted great interest [6–10]. The Rashba effect can be utilized in important spintronics applications, such as the spin-based transistor [11]. The effects of large Rahba spin splitting in $A^5B^6C^7$ by angle-resolved photoemission spectroscopy (ARPES) has been observed [6,12–15].

The experimental studies and first principle calculations have increasingly been employed to explore the electronic and crystal structure of these compounds. Zhuang et al. [10] investigated the Rashba spin splitting in the spin orbit coupling (SOC) band structure, density of state and phonon properties of single layer SbTeI using VASP code. Akrapet et al. [15] investigated the optical properties and Raman spectra of BiTeBr and BiTeCl single crystal using chemical vapor transport and topotactic methods. Fiedler et al. [9] investigated the surface structural and electronic properties of the semiconductors BiTeX (X = Cl, Br, I) using the various techniques. Moreschiniet et al. [16] investigated the surface states using the QUANTUM-ESPRESSO package. Dubeyet et al. [17] observed that SbTeI showed metallic behavior from 4 K to 300 K and semiconducting behavior at higher temperature

CONTACT Amirullah M. Mamedov mamedov@bilkent.edu.tr
Color versions of one or more of the figures in the article can be found online at www.tandfonline.com/gfer.

(>300 K). Landolt et al. [18] investigated the three dimensional bulk states and the two dimensional surface states using the GGA. Kulbachinskiiet et al. [19] investigated the thermoelectric and galvanomagnetic properties using the Bridgman method. Ma et al. [20] examined the energetic stability electronic and phonon properties of BiTeX (X = Br, I) monolayers using ab initio calculations. Zhu et al. [21] calculated the electronic band structure of BiTeCl in the absence of spin orbit coupling using the WIEN2k package.

In the present work, we aimed at providing some additional information to the existing data on the physical properties of $A^5B^6C^7$ compounds by using ab initio total energy calculations, and we especially focused on the electronic, mechanical, and optical properties. To our knowledge, the mechanical properties for SbTeI and BiSI compounds, optical properties of dielectric functions (except for the part real and imaginary of BiSI) have not been reported in detail for these compounds so far.

2. Method of calculation

In all of our calculations that were performed using the ab-initio total-energy and molecular-dynamics program VASP (Vienna ab-initio simulation program) [22–25] that was developed within the density functional theory (DFT) [26], the exchange-correlation energy function is treated within the GGA (generalized gradient approximation) by the density functional of Perdew et al. [27]. The potentials used for the GGA calculations take into account the $6s^26p^3$ valence electrons of each Bi-, $5s^25p^3$ valence electrons of each Sb-, $5s^25p^4$ valence electrons of each Te-, $3s^23p^4$ valence electrons of each S-, $3s^23p^5$ valence electrons of each Cl-, and $4s^24p^5$ valence electrons of each Br-atoms. When including a plane-wave basis up to a kinetic-energy cutoff equal to 10.72 Ha (for SbTeI), 12.85 Ha (for BiTeI), 12.87 Ha (for BiTeCl), 22.18 Ha (for BiTeBr), and 20.47 Ha (for BiSI), the properties investigated in this work are well converged. The Brillouin-zone integration was performed using special k points sampled within the Monkhorst-Pack scheme [28]. We found that a mesh of $11 \times 11 \times 4$, $8 \times 8 \times 4$, $9 \times 9 \times 3$, $11 \times 11 \times 6$, and $8 \times 16 \times 7$ k points for SbTeI, BiTeI, BiTeCl, BiTeBr and BiSI, respectively, was required to describe the structural, mechanical, electronic, and optical properties. This k-point mesh guarantees a violation of charge neutrality less than 0.008e. Such a low value is a good indicator for an adequate convergence of the calculations.

The positions corresponding to the $A^5B^6C^7$ (A = Sb, Bi; B = Te, Se; S; C = I, Br, Cl) compounds have been obtained from experimental data [30–39]. The atomic positions belonging to these compounds are given in Table 1. The crystal structures of BiTeI and BiTeBr compounds are the same. Both of these compounds crystallize in a trigonal structure with space groups P3m1 (156), and the unit cell of the crystal structures contains 1 molecule and 3 atoms. BiTeCl has a hexagonal crystal structure with space groups $P6_3mc$ (186), and the unit cell of the crystal structure contains 2 molecules and 6 atoms. SbTeI and BiSI compounds crystallize in monoclinic and orthorhombic structures with space groups C2/m (12) and Pnma(62), respectively. The unit cell each of these compounds contains 4 molecules and 12 atoms.

3. Results and discussion

We have used the experimental structural parameter in the first step of our calculation, but these values may not always give the correct result. Therefore, the geometric optimization

Table 1. The calculated equilibrium lattice parameters (a, b, and c in Å) and electronic band gaps together with the theoretical and experimental values for $A^5B^6C^7$ (A = Sb, Bi; B = Te, Se; S; C = I, Br, Cl) compounds.

Lattice	Material	a	b	c	V_0 (Å^3)	E_g(eV)	Refs.
Trigonal P3m1 (156)	BiTeI	4.425		7.227	122.53	1.24	Present
A: 1a (0.0, 0.0, z)		4.339		6.854	111.81		Exp. [29]
B: 1b (1/3, 2/3, z)		4.437		7.433	127.04	0.43	PAW-PBE [30]
C: 1c (2/3, 1/3, z)		4.284		7.021	111.63	0.21	PAW-PBE-D2 [30]
						0.38	APW+lo-PBE [6]
						0.36	Exp. [31]
						0.26	Exp. [32]
		4.328		6.906		0.8	UPPW-PBE [33]
	BiTeBr	4.351		7.064	115.79	1.09	Present
		4.266		6.486	102.25		Exp. [34]
		4.25		6.596		1.1	UPPW-PBE [33]
Hexagonal $P6_3mc$ (186)	BiTeCl	4.295		13.343	213.14	1.38 (I)	Present
A; B: 2b (2/3, 1/3, z)		4.243		12.397	193.31		Exp. [29]
C: 2a (0, 0, z)		4.241		12.403			Exp. [35]
		4.213		12.531		1.2	UPPW-PBE [33]
Monoclinic C2/m (12)	SbTeI	14.903	4.299	9.778	472.09	0.89 eV (I)	Present
A;B;C: 4i (x,0,z)		13.701	4.242	9.201	417.72		Exp. [36]
Orthorhombic Pnma (62)	BiSI	8.926	4.207	11.023	413.92	1.88 (I)	Present
A;B;C: 4c (x,1/4,z)		8.45	4.139	10.147	354.88		Exp. [37]
		8.44	4.13	10.26		1.78 (I); 1.82 (D)	PAW-PBE [38]
						1.57 (I)	FP-LAPW [39]
						1.59	Exp. [40]

process is performed to detect that the structure is the correct structure. The lattice parameters obtained as a result of optimization are given in Table 1 along with the experimental and theoretical values, and these parameters are used for the electronic, mechanical, and optical calculations. The obtained lattice parameters for the $A^5B^6C^7$ (A = Sb, Bi; B = Te, Se; S; C = I, Br, Cl) compounds are in agreement with the experimental and theoretical values [29, 30, 33–38].

The elastic constants calculated with the strain-stress relationship [41] for $A^5B^6C^7$ compounds are given in Table 2 along with the theoretical values. As can be seen in Table 2, the value of the calculated elastic constants for BiTeI compound is in good agreement with the theoretical values. However, the value of the calculated elastic constant C_{33} for BiTeBr is higher than the theoretical value, but the calculated C_{33} (C_{44}) value for BiTeCl is lower (higher) than the theoretical value. It is seen that all the

Table 2. The calculated elastic constants (in GPa) for $A^5B^6C^7$ (A = Sb, Bi; B = Te, Se; S; C = I, Br, Cl) compounds.

Compound	Refs.	C_{11}	C_{12}	C_{13}	C_{15}	C_{22}	C_{23}	C_{25}	C_{33}	C_{35}	C_{44}	C_{46}	C_{55}	C_{66}
BiTeI	Present	57.8	16.1	25.5					46.2		20.9			
	UPPW-PBE [33]	60.4	14.1	20.2					42		24.3			
BiTeBr	Present	59.8	18.4	23.2					54.8		20.6			
	UPPW-PBE [33]	59.3	14.9	13.1					28.6		14.9			
BiTeCl	Present	74.2	21.4	32.4					55.8		26.5			
	UPPW-PBE [33]	56.6	20.8	47.6					96.6		1.7			
SbTeI	Present	49.5	32.4	19.4	5.9	66.1	12.1	15.6	67.4	−16.1	37.6	16.5	19.3	30.1
BiSI	Present	77.3	16.9	20.2		80.6	43.1		62.6		16.1		42.9	25.2

compounds under zero pressure provide the mechanical stability criteria [42–46]. The elastic constants C_{11}, C_{22}, and C_{33} measure the a-, b-, and c-direction resistance to linear compression, respectively. The C_{11} value for BiTeI, BiTeBr, and BiTeCl compounds is higher than the C_{33} value. Therefore, the a-direction of these compounds is less compressible. The C_{22} value for the BiSI compoundis higher than the C_{11} and C_{33} values while the C_{33} value for SbTeI compound is higher than C_{11} and C_{33} values. At that, the c-direction for SbTeI and the b- direction for BiSI are less compressible. C_{44}, C_{55}, and C_{66} values show the shear distortion resistance in the (100), (010), and (001) plane, respectively. The SbTeI compound from these compounds has higher C_{44} and C_{66} values. BiSI compound also has a higher C_{55} value.

The other polycrystalline elastic properties (Young's modulus, Poisson's ratio, sound velocities, and Debye temperature) from the polycrystalline bulk modulus and isotropic shear modulus obtained by using the Voigt- Reuss-Hill (VRH) approach [47–49] have been calculated, and have been given in Table 3 along with the theoretical values. It is seen that the values of BiTeI and BiTeBr are in good agreement with the theoretical values, but the values of BiTeCl are not in good agreement with the theoretical values (except for the bulk modulus). The isotropic shear modulus and bulk modulus are a measure of the hardness of a solid. The bulk modulus and isotropic shear modulus for BiSI compound are higher than the other composite values. Young's modulus is defined as the ratio of stress and strain, and used to provide a measure of the stiffness of the solid. Here, the most high Young's modulus belongs to BiSI compound. Therefore, this compound is harder than the other compounds. The value of the Poisson's ratio is indicative of the degree of directionality of the covalent bonds. The value of Poisson's ratio is small ($\upsilon = 0.1$) for covalent materials, whereas for ionic materials a typical value of υ is 0.25 [50–51]. As can be seen in Table 3, the ionic contribution to inter atomic bonding for these compounds is dominant. According to the criterion in refs. [52, 53], a material is brittle (ductile) if the B / G ratio is less (high) than 1.75. The value of the B / G of BiTeI, BiTeCl, and BiSI compounds is higher than 1.75. Hence, these compounds behave in a ductile manner. The value of the B / G of BiTeBr and SbTeI compounds is also less than 1.75. Hence, these compounds behave in a brittle manner. The elastic anisotropy is given by the percentage of anisotropy in the compression (A_B) and shear (A_G). For crystals, these values can range from zero (isotropic) to 100% representing the maximum anisotropy [50, 54,55]. The SbTeI among these compounds has high shear and bulk anisotropies

Table 3. The calculated isotropic bulk modulus (B, in GPa), shear modulus (G, in GPa), Young's modulus (E, in GPa), Poisson's ratio, anisotropic factors, sound velocities (υ_t, υ_l, υ_m), and the Debye temperature for $A^5B^6C^7$ (A = Sb, Bi; B = Te, Se; S; C = I, Br, Cl) compounds.

Compound	Reference	B	G	E	υ	B/G	A_B	A_G	A^U	υ_t	υ_l	υ_m	θ_D
BiTeI	Present	32.8	18.1	45.9	0.27	1.81	0.02	3.58	0.37	1697	3010	1888	163
	UPPW-PBE [33]	30	18.8	46.6	0.24	1.6	0.72	14.75	1.74	1653	2831	1834	163
BiTeBr	Present	33.8	19.6	49.3	0.26	1.72	0.002	0.51	0.05	1811	3167	2012	177
	UPPW-PBE [33]	24	13.5	38.3	0.23	1.54	6.1	13.05	1.63	1537	2607	1703	155
BiTeCl	Present	41.8	22.8	57.9	0.27	1.83	0.19	4.23	0.45	1983	3529	2207	200
	UPPW-PBE [33]	42.9	7	20	0.42	6.1	14.37	49.4	10.1	1047	2856	1189	111
SbTeI	Present	30.2	22.4	53.9	0.2	1.35	14.24	13.2	1.85	2057	3368	2272	199
BiSI	Present	42	24	60.5	0.26	1.75	0.83	9.17	1.03	2016	3540	2241	205

(see Table 3). A concept of the universal anisotropy index, which is another way of measuring the elastic anisotropy, was introduced by Ranganathan et al. [56,33]:

$$A^U = 5\frac{G_V}{G_R} + \frac{B_V}{B_R} - 6 \quad (1)$$

Here, $A^U = 0$ represents locally isotropic crystals and $A^U > 0$ denotes the extent of crystal anisotropy. SbTeI compound has strong anisotropy because the SbTeI among these compounds has a high A^U value. The Debye temperature and sound velocity [57–59] calculated for these compounds are given in Table 2 along with the theoretical values. The least Debye temperature belongs to the SbTeI compound, but the values of other compounds are also close to this value. Usually, the Debye temperature is low for soft materials, but is high for rigid materials. Consequently, these compounds can be called soft materials. The highest Debye temperature among these compounds belongs to the BiSI compound, and this compound is rigid material accord to the other compounds.

The calculated band structures and partial densities of states of $A^5B^6C^7$ compounds along high symmetry directions using the lattice constants obtained are shown in Fig. 1. The Fermi energy level has been taken as zero. As can be seen in Fig. 1, BiTeI, BiTeCl, SbTeI, and BiSI compounds have indirect band gap, which are 1.24 eV (from the nearly A point between A and T to A high symmetry point), 1.38 eV (from the nearly G point between G and K to G point), 0.89 eV (from the nearly G point between G and Z to Z point), and 1.88 eV (from nearly the Y point between S and Y point to nearly the T point between T and Z point), respectively. BiTeBr compound also has a direct band gap, which is 1.09 eV (ahigh symmetry point). The obtained band gap values for these compounds have been summarized in Table 1 along with the experimental and theoretical values. The obtained band gap value for BiTeI compound is too high for the experimental and theoretical values [6, 29–31], but this value is a little higher than the theoretical value [33]. The values of BiTeBr, BiTeCl, and BiSI compounds are in agreement with the experimental and theoretical values [33, 36, 38–40]. Unfortunately, there are no theoretical and experimental results for comparing with the band gap value of SbTeI compound. The materials with the narrow band gap are important for mid-infrared optoelectronic applications [60–61]. In this respect, the semiconductors with the narrow band gap from these compounds can be alternative for mid-infrared applications. The density of states of these compounds is similar to one another as shown in Fig. 1. In this figures, the lowest valance bands for these compounds are dominated by d states that occur between approximately −24 and −22 eV. The mid-level valance bands are also dominated by s states that occur between approximately −15 and −8 eV. The highest occupied valance bands and the lowest unoccupied conduction bands are dominated by p states. The d and s states also contributeto the highest occupied valance and the lowest unoccupied conduction bands, but the values of the density of states of these states are rather small compared to p states. Therefore, the ionic bonding structure for these compounds dominates because of the p states that play a role in the transmission.

We first calculated the real and imaginary parts of $\varepsilon(\omega) = \varepsilon_1(\omega) - i\varepsilon_2(\omega)$ for the $A^5B^6C^7$ compounds (except for the part real and imaginary of BiSI) along the x- and z- direction using Kramers-Kroning transformation [62]. Figure 2 shows the real and imaginary of $\varepsilon(\omega)$ together with the energy loss function. The results obtained showa manner similar to our recent works [63,64]. The ε_1 behaves mainly as a classical oscillator. The ε_1 parts (for $d\varepsilon_1$

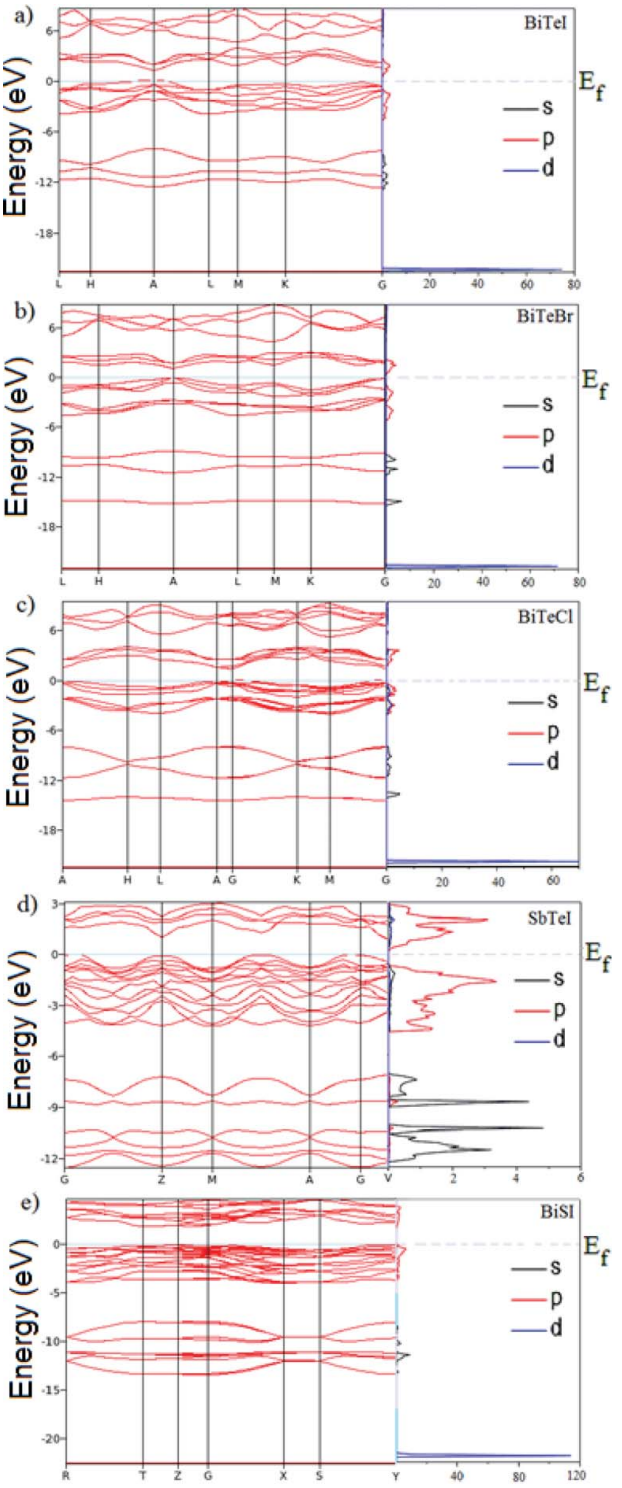

Figure 1. Energy band structures and projected density of states for (a) BiTeI, (b) BiTeBr, (c) BiTeCl, (d) SbTeI, and (e) BiSI compounds.

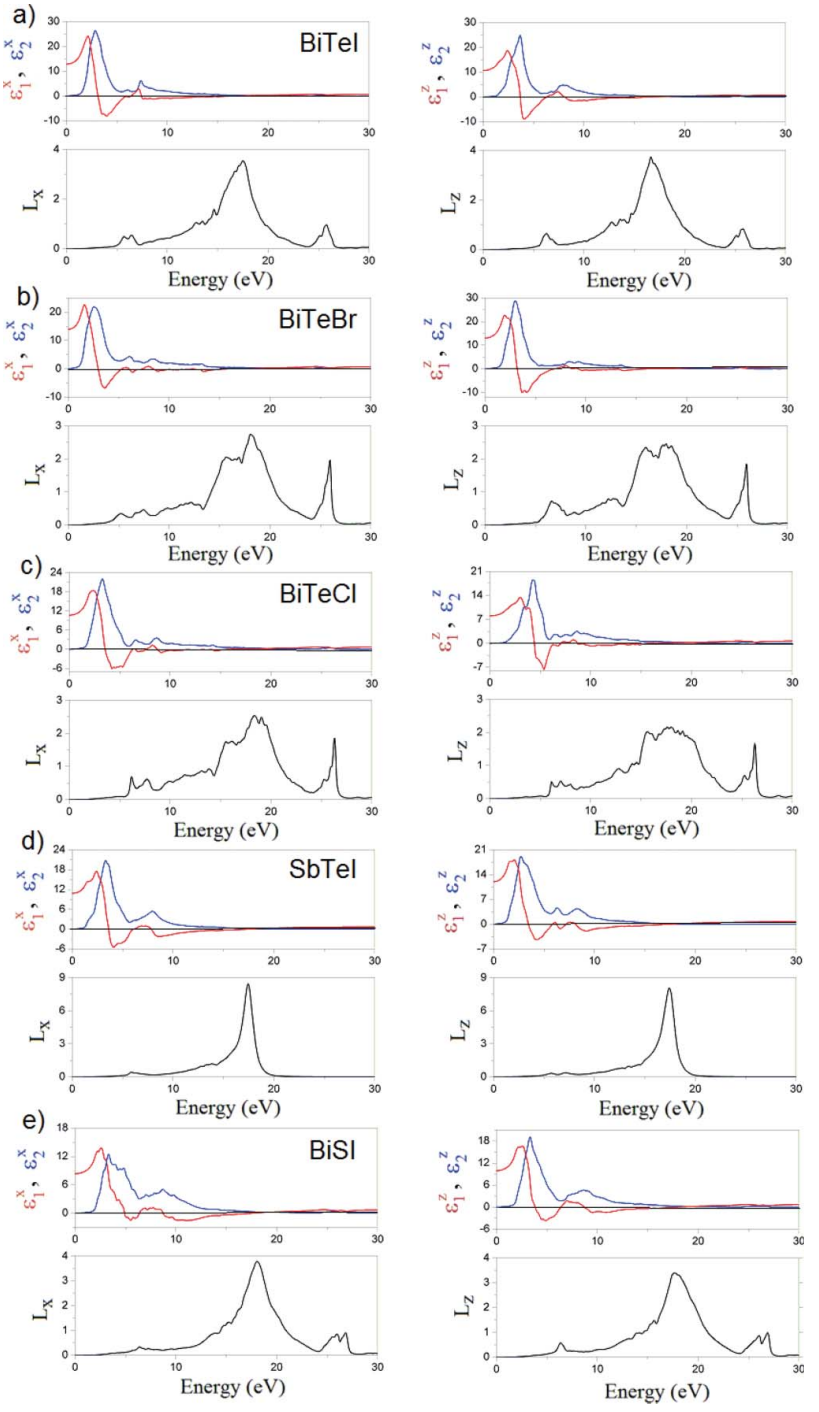

Figure 2. Energy spectra of the dielectric function $\varepsilon = \varepsilon_1 - i\varepsilon_2$ and energy-loss function (L) along the x- and z-axes for (a) BiTeI, (b) BiTeBr, (c) BiTeCl, (d) SbTeI, and (e) BiSI compounds.

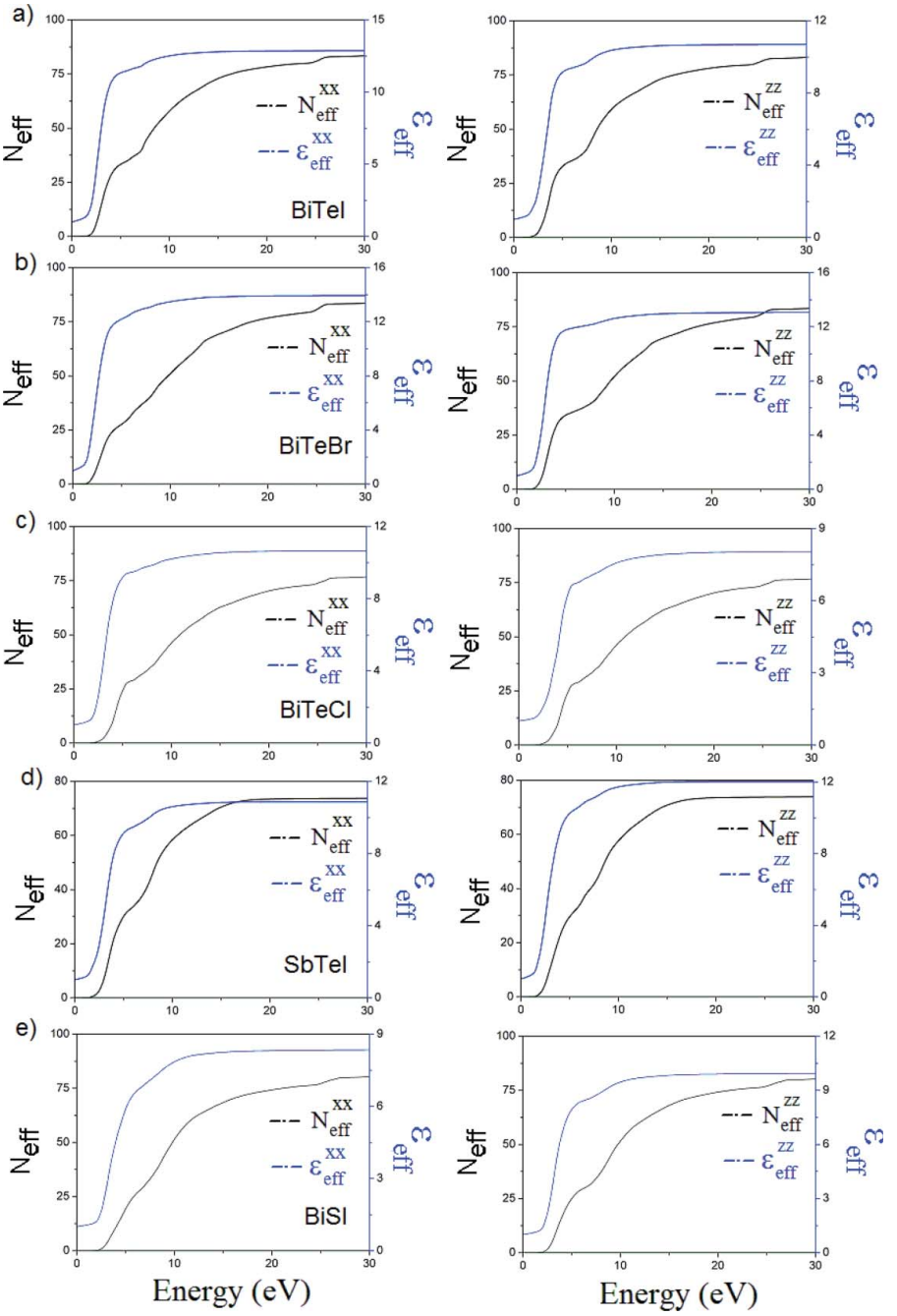

Figure 3. Energy spectra of N_{eff} and ε_{eff} along the x- and z- axes for (a) BiTeI, (b) BiTeBr, (c) BiTeCl, (d) SbTeI, and (e) BiSI compounds.

$/\,dE > 0$ and $d\varepsilon_1\,/\,dE < 0$) of these compounds are equal to zero in the energy region between 2.9 eV and 17 eV (see Table 4). The peaks of the ε_2 parts are related to the optical transitions from the valance bands to the conduction band. The maximum peak values of $\varepsilon_2^x(\varepsilon_2^z)$ for BiTeI, BiTeBr, BiTeCl, SbTeI, and BiSI compounds around 2.85 (3.70) eV, 2.55

Table 4. Some of principal features and singularities of the linear optical responses for $A^5B^6C^7$ (A = Sb, Bi; B = Te, Se; S; C = I, Br, Cl) compounds.

Material	$\varepsilon_1(eV)$	$d\varepsilon_1/dE<0$			$d\varepsilon_1/dE>0$			$\varepsilon_2(eV)$	
BiTeI	ε_1^x	3.13		7.45	6.37		16.44	$\varepsilon_{2,\max}^x$	2.85
	ε_1^z	3.70		8.14	6.26		16.39	$\varepsilon_{2,\max}^z$	3.70
BiTeBr	ε_1^x	2.96	6.05	8.48	5.28	7.35	15.71	$\varepsilon_{2,\max}^x$	2.55
	ε_1^z	3.20		9.31	6.88		15.83	$\varepsilon_{2,\max}^z$	2.96
BiTeCl	ε_1^x	3.57	6.57	8.75	6.22	7.60	15.78	$\varepsilon_{2,\max}^x$	3.34
	ε_1^z	4.44		8.76	7.03		15.66	$\varepsilon_{2,\max}^z$	4.26
SbTeI	ε_1^x	3.62		7.86	6.03		17.26	$\varepsilon_{2,\max}^x$	3.33
	ε_1^z	3.47	6.21	8.16	5.85	7.17	17.19	$\varepsilon_{2,\max}^z$	2.71
BiSI	ε_1^x	4.93		8.75	6.32		17.61	$\varepsilon_{2,\max}^x$	3.30 3.0 [39]
	ε_1^z	3.88		8.75	6.32		17.44	$\varepsilon_{2,\max}^z$	3.30 3.5 [39]

(2.96) eV, 3.34 (4.26) eV, 3.33 (2.71) eV, and 3.30 (3.30) eV, respectively. As can be seen in Table 4, the$\varepsilon_2^x\left(\varepsilon_2^z\right)$ values of BiSI compound are in agreement with the theoretical values [39]. The function $L(\omega)$ describes the energy loss of fast electrons traversing the material. The sharp maxima in the energy-loss function are associated with the existence of plasma oscillations [65]. As can be seen in figure 2, the L_x (L_z) curves have a maximum near 17.47 (16.61) eV for BiTeI, 18.01 (17.96) eV for BiTeBr, 18.37 (17.62) eV for BiTeCl, 17.44 (17.41) eV for SbTeI, and 18.02 (17.67) eV for BiSI. The known sum rules can be used to determine some quantitative parameters, as well as the effective number of the valence electrons per unit cell N_{eff} and the effective optical dielectric constant ε_{eff} [66]. The calculated effective number of valence electrons N_{eff} and the effective dielectric constant ε_{eff} are given in Fig. 3. The effective number of valance electrons per unit cell, N_{eff} (contributing in the interband transitions), reaches the saturation value at energies above 25 eV. This means that deep-lying valence orbitals participate in the interband transitions as well. The effective optical dielectric constant ε_{eff} reaches a saturation value at approx. 10 eV. This means that the greatest contribution to ε_{eff} arises from interband transitions between 0.5 eV and 10 eV (see Fig. 3)

Conclusion

The ternary chalcohalides formed from the group 5-6-7 elements ($A^5B^6C^7$ where A = Bi, Sb; B = S, Se, Te; C = I, Br, Cl) constitute a class of materials exhibiting a wide range of interesting and potentially useful semiconducting and ferroelectric properties. Some compounds of this class are topological insulators (BiTeI, SbTeI, and BiSeI) and have recently been attractinga great deal of interest as a potential spintronic material due to the emergence of giant Rashba-type spin splitting in their band structures. In the present paper, we focus on general principles governing the emergence of valence electronic states in different $A^5B^6C^7$ and their electronic band structure, optical, and elastic properties for the ABC compounds using the density functional methods in a generalized gradient approximation.The lattice parameters of considered compounds have been calculated. The second-order elastic constants have been calculated, and the other related quantities such as Young's modulus, shear modulus, Poisson's ratio, anisotropy factor, sound velocities, and Debye temperature have also been estimated in the present work. The electronic band structures and the partial densities of

states corresponding to the band structures are presented and analyzed. The real and imaginary parts of dielectric functions and hence the optical constant such as energy-loss function, the effective number of valance electrons and the effective optical dielectric constant are calculated. Our structural estimation and some other results are in agreement with the available experimental and theoretical data.

Funding

This work is supported by the projects DPT-HAMIT and NATO-SET-193, and one of the authors (Ekmel Ozbay) also acknowledges partial support from the Turkish Academy of Sciences.

References

1. E. I. Gerzanich and V. M. Fridkin, *Segnetoelektrikitipa $A^5B^6C^7$*. Nauka, Moskwa p. 114 1982.
2. J. Fenner, A. Rabenau, and G. Trageser, *Adv. Inorg. and Radiochemistry* V. 23, Acad. Press. New York, pp. 329–416 1980.
3. B. A. Popovkin, Physico-chemical fundamentals of the control synthesis of sulpho-iodide of antimony and other chalcogeno-(oxo)-halogenides of antimony and bismuth. Doctoral thesis, M: MSU, p. 349 1983.
4. V. V. Soboley, E. V. Pesterev, and V. V. sobolev, Dielectric permittivity of BiTeI. *Inorg Mater.* **40**, 128–129 (2004).
5. M. B. Babanly, J. C. Tedenac, Z. S. Aliyev, and D. V. Balitsky, Phase equilibriums and thermodynamic properties of the system Bi-Te-I. *J of Alloys and Comp.* **481**, 349–353 (2009).
6. K. Ishizaka, M. S. Bahramy, H. Murakawa, M. Sakano, T. Shimojima, T. Sonobe, K. Koizumi, S. Shin, H. Miyahara, A. Kimura, K. Miyamoto, T. Okuda, H. Namatame, M. Taniguchi, R. Arita, N. Nagaosa, K. Kobayashi, Y. Murakami, R. Kumai, Y. Kaneko, Y. Onose, and Y. Tokura, Giant Rashba-type spin splitting in bulk BiTeCl. *Nat Mater.* **10**, 521–526 (2011).
7. S. V. Eremeev, I. A. Nechaev, Y. M. Koroteev, P. M. Echenique, and E. V. Chulkov, Ideal two-dimensional electron systems with a giant Rashba-type spin splitting in real materials: surfaces of bismuth tellurohalides. *Phys Rev Lett.* **108**, 246802 (2012).1–5.
8. H. Murakawa, M. S. Bahramy, M. Tokunaga, Y. Kohama, C. Bell, Y. Kaneko, N. Nagaosa, H. Y. Hwang, and Y. Tokura, Detection of berry's phase in a bulk Rashba semiconductor. *Science* **342**, 1490–1493 (2013).
9. S. Fiedler, T. Bathon, S. V. Eremeev, O. E. Tereshchenko, K. A. Kokh, E. V. Chulkov, P. Sessi, H. Bentmann, M. Bode, and F. Reinert, Termination-dependent surface properties in the giant-Rashba semiconductors BiTeX (X = Cl, Br, I). *Phys Rev B.* **92**, 235430.1–10 (2015).
10. H. L. Zhuang, V. R. Cooper, H. Xu, P. Ganesh, R. G. Hennig, and PRC Kent, Rashba effect in single layer antimony telluroiodide SbTeI. *Phys Rev B.* **92**, 115302 (2015).1–5.
11. S. Datta and B. Das, Electronic analog of the electro−optic modulator. *Appl Phys Lett.* **56**, 665–667 (1990).
12. A. Crepaldi, L. Moreschini, G. Autes, C. Tournier-Colletta, S. Moser, N. Virk, H. Berger, P. Bugnon, Y. J. Chang, K. Kern, A. Bostwick, E. Rotenberg, O. V. Yazyev, and M. Grioni, Giant ambipolar Rashba effect in the semiconductor BiTeI. *Phys Rev Lett.* **109**, 096803 (2012).1–5.
13. G. Landolt, S. V. Eremeev, Y. M. Koroteev, B. Slomski, S. Muff, T. Neupert, M. Kobayashi, V. N. Strocov, T. Schmitt, Z. S. Aliev, M. B. Babanly, I. R. Amiraslanov, E. V. Chulkov, J. Osterwalder, and J. H. Dill, Disentanglement of surface and bulk Rashba spin splittings in noncentrosymmetric BiTeI. *Phys Rev Lett.* **109**, 116403 (2012).
14. M. Sakano, M. S. Bahramy, A. Katayama, T. Shimojima, H. Murakawa, Y. Kaneko, W. Malaeb, S. Shin, K. Ono, H. Kumigashira, R. Arita, N. Nagaosa, H. Y. Hwang, Y. Tokura, and K. Ishizaka, Strongly spin-orbit coupled two-dimensional electron gas emerging near the surface of polar semiconductors. *Phys Rev Lett.* **110**, 107204.1–5 (2013).

15. A. Akrap, J. Teyssier, A. Magrez, P. Bugnon, H. Berger, A. B. Kuzmenko, D. van der Marel, Optical properties of BiTeBr and BiTeCl. *Phys Rev B.* **90**, 035201.1–6 (2014).
16. L. Moreschini, G. Autès, A. Crepaldi, S. Moser, J. C. Johannsen, K. S. Kim, H. Berger, P. Bugnon, A. Magrez, J. Denlinger, E. Rotenberg, A. Bostwick, O. V. Yazyev, and M. Grioni, Bulk and surface band structure of the new family of semiconductors BiTeX (X = I, Br, Cl). *J of Electron Spectroscopy and Related Phenomena* **201**, 115–120 (2015).
17. H. K. Dubey, L. P. Deshmukh, D. E. Kshirsagar, M. Sharon, and M. Sharon, Synthesis and study of electrical properties of SbTeI. *Advances in Physical Chemistry* **2014**, 1–6 (2014).
18. G. Landolt, S. V. Eremeev, O. E. Tereshchenko, S. Muff, B. Slomski, K. A. Kokh, M. Kobayashi, T. Schmitt, V. N. Strocov, J. Osterwalder, E. V. Chulkov, and J. H. Dil, Bulk and surface Rashba splitting in single termination BiTeCl. *New J of Phys.* **15**, 085022.1–11 (2013).
19. V. A. Kulbachinskii, V. G. Kytin, Z. V. Lavrukhina, A. N. Kuznetsov, and A. V. Shevelkov, Galvanomagnetic and thermoelectric properties of BiTeBr and BiTeI single crystal and their electronic structure. *Semiconductors* **44**, 1548–1553 (2010).
20. Y. Ma, Y. Dai, W. Wei, X. Li, and B. Huang, Emergence of electric polarity in BiTeX (X = Br and I) monolayers and the giant Rashba spin splitting. *Phys Chem Chem Phys.* **16**, 17603–17609 (2014).
21. Z. Zhu, Y. Cheng, and Schwingenschlögl U: Orbital-dependent Rashba coupling in bulk BiTeCl and BiTeI. *New J of Phys.* **15**, 023010.1–10 (2013).
22. G. Kresse and J. Hafner, Ab initio molecular dynamics for liquid metals. *Phys Rev B.* **47**, 558–561 (1993).
23. J. Kresse G andFurthmüller, Ab-initio total energy calculations for metals and semiconductors using a plane-wave basis set. *Comput Mater Sci.* **6**, 15–50 (1996).
24. G. Kresse and D. Joubert, From ultrasoft pseudopotentials to the projector augmented-wave method. *Phys Rev B.* **59**, 1758–1775 (1999).
25. G. Kresse and J. Furthmüller, Efficient iterative schemes for ab initio total- energy calculations using a plane-wave basis set. *Phys Rev B.* **54**, 11169–11186 (1996).
26. P. Hohenberg and W. Kohn, Inhomogeneous Electron Gas. *Phys Rev.* **136**, A1133–A1138 (1964).
27. J. P. Perdew and S. Burke, Ernzerhof M. Generalized gradient approximation made simple. *Phys Rev Lett.* **77**, 3865–3868 (1996).
28. H. J. Monkhorst and J. D. Pack, Special points for Brillouin-zone integrations. *Phys Rev B.* **13**, 5188–5192 (1976).
29. A. Shevelkov, E. Dikarev, R. Shpanchenko and B. Popovkin, Crystal structures of bismuth tellurohalides BiTe*X*(*X* = Cl, Br, I) from X-Ray powder diffraction data. *J Solid State Chem.* **114**, 379–384 (1995).
30. S. G. Kılıç and Ç Kılıç, Crystal and electronic structure of BiTeI, AuTeI, and PdTeI compounds: A dispersion-corrected density-functional study. *Phys Rev B.* **91**, 2452041–12 (2015).
31. J. S. Lee, GAH Schober, M. S. Bahramy, H. Murakawa, Y. Onose, R. Arita, N. Nagaosa, and Y. Tokora, Optical Response of Relativistic Electrons in the Polar BiTeI Semiconductor. *Phys Rev Lett.* **107**, 117401.1–5 (2011).
32. M. Skano, J. Miyawaki, A. Chainani, Y. Takata, T. Sonobe, T. Shimojima, M. Oura, S. Shin, M. S. Bahramy, R. Arita, N. Nagaosa, H. Murakawa, Y. Kaneko, Y. Tokura, and K. Ishizaka, Three-dimensional bulk band dispersion in polar BiTeI with giant Rashba-type spin splitting. *Phys Rev B.* **86**, 085204 (2012).
33. S. Zhou, J. Long and W. Huang, Theoretical prediction of the fundamental properties of ternary bismuth tellurohalides. *Materials Sciences in Semiconductors Processing* **27**, 605–610 (2014).
34. J. A. Sans, F. J. Manjon, ALJ Pereira, R. Vilaplana, O. Gomis, A. Segura, A. Munoz, P. Rodriguez-Hernandez, C. Popescu, C. Drasar, and P. Rulevas, Structural, vibrational, and electrical study of compressed BiTeBr. *Phys Rev B.* **93**, 024110.1–11 (2016).
35. J. Jamimovic, X. Mettan, A. Pisoni, R. Gaal, S. Katrych, L. Demko, A. Akrap, L. Forro, H. Berger, P. Bugnon, and A. Magrez, Enhanced low-temperature thermoelectrical properties of BiTeCl grown by topotactic method. *ScriptaMaterialia* **76**, 69–72 (2014).
36. A. G. Papazoglou and P. J. Rentzeperis, The Crystal structure of antimony telluroiodide, SbTeI. *Zeitschrift für Kristallographie* **165**, 159–167 (1983).

37. F. Demartin, C. Gramaccioli, and I. Campostrini, Demichelete-(I), BiSI, a new mineral from la fossa crater, Vulcano, Aeolian Islands, Italy. *Mineral. Mag.* **74**, 141–145 (2010).
38. A. M. Ganose, K. T. Butler, A. Walsh, and D. O. Dcanlon, Relativistic electronic structure and band alignment of BiSI and BiSeI: candidate photovoltaic materials. *J Mater Chem A.* **4**, 2060–2068 (2016).
39. A. Audzijonis, R. Zaltauskas, R. Sereika, L. Zigas, and A. Reza, Electronic structure and optical properties of BiSI crystal. *J of Phys and Chems of Solids* **71**, 884–891 (2010).
40. S. A. Park, M. Y. Kim, J. Y. Lim, B. S. Park, J. D. Koh, and W. T. Kim, Optical Properties of Undoped and V-Doped $V^A-VI^A-VII^A$ Single Crystals. *Phys Status Solidi (b)* **187**, 253–260 (1995).
41. Y. a. Le Page and P. Saxe, Symmetry-general least-squares extraction of elastic coefficients from ab initio total energy calculations. *Phys Rev B.* **63**, 174103.1–174103.8 (2001).
42. J. P. Watt, Hashin-Shtrikman bounds on the effective elastic moduli of polycrystals with orthorhombic symmetry. *J Appl Phys.* **50**, 6290–6295 (1979).
43. J. P. Watt, Hashin-Shtrikman bounds on the effective elastic moduli of polycrystals with monoclinic symmetry. *J Appl Phys.* **51**, 1520–1524 (1980).
44. J. P. Watt, L. Peselnick, Clarification of the Hashin-Shtrikman bounds on the effective elastic moduli of polycrystals with hexagonal, trigonal, and tetragonal symmetries. *J Appl Phys.* **51**, 1525–1531 (1980).
45. J. F. Nye, *Physical properties of crystals*. Oxford, Oxford University Press, 1985.
46. Z. Wu, E. Zhao, H. Xiang, X. Hao, X. Lui, and J. Meng, Crystal structures and elastic properties of superhard IrN_2 and IrN_3 from first principles. *Phys Rev B.* **76**, 054115.1–15 (2007).
47. W. Voight, *Lehrbook der kristallphysik Leipsig*. Teubner, p. 962 1928.
48. A. Reuss, Berechnung der Fließgrenze von Mischkristallen auf Grund der Plastizitatsbedingung für Einkristalle. *Z Angew Math Mech.* **9**, 49–58 (1929).
49. R. Hill, The elastic behavior of crystalline aggregate. *Proc Phys Soc London Sect A.* **65**, 349–354 (1952).
50. V. V. Bannikov, I. R. Shein, and A. L. Ivanovskii, Electronic structure, chemical bonding and elastic properties of the first thorium-containing nitride perovskite $TaThN_3$. *Phys Stat Sol (RRL).* **3**, 89–91 (2007).
51. H. Koc, A. Yildirim, E. Tetik, and E. Deligoz, Ab initio calculation of the structural, elastik, electronic, and linear optical properties of ZrPtSi and TiPtSi ternary compounds. *Computational Materials Science* **62**, 235–242 (2012).
52. A. L. Shein IR andIvanovskii, Elastic properties of mono-and polycrystalline hexagonal AlB_2-like diborides of s, p and d metals from first-principles calculations. *J Phys Considens Matter.* **20**, 415218.1–415218.9 (2008).
53. F. Pogh, XCII. Relations between the elastic moduli and the plastic properties of polycrystalline pure metals. *Philos Mag.* **45**, 823–843 (1954).
54. H. Fu, D. Li, F. Peng, T. Gao, and X. Cheng, Ab initio calculations of elastic constants and thermodynamic properties of NiAl under high pressures. *Comput Mater Sci.* **44**, 774–778 (2008).
55. V. Tvergaard and J. W. Hutchinson, Microcracking in Ceramics Induced by Thermal Expansion or Elastic Anisotropy. *J Am Chem Soc.* **71**, 157–166 (1988).
56. SIand Ranganathan, M. Ostoja-Starzewski, Universal Elastic Anisotropy Index. *Phys Rev Lett.* **101**, 055504 (2008).
57. I. Johnston, G. Keeler, R. Rollins, and S. Spicklemire, *Solids state physics simulations, the consortium for upper level physics software*. Wiley, New York, 1996.
58. O. L. Anderson, A simplified method for calculating the Debye temperature from elastic constants. *J Phys Chem Solids.* **24**, 909–917 (1963).
59. E. Schreiber, O. L. Anderson, and N. Soga, *Elastic constants and their measurements*. McGraw-Hill, New York, 1973.
60. D. A. McGill TC andCollins, Prospect for the future of narrow band gap materials. *Semicond Sci Technol.* **8**, 51–53 (1993).
61. S. Krishnamurthy, A. B. Chen, and A. Sher, Near band edge absorption spectra of narrow gap III-V semiconductors alloys. *J Appl Phys.* **80**, 4045–4048 (1996).

62. H. R. Philipp and H. Ehrenreich, Optical properties of semiconductors. *Phys Rev.* **129**, 1550–1560 (1963).
63. H. Koc, A. M. Mamedov, E. Deligoz, and H. Ozışık, First principle prediction of the elastic, electronic, and optical properties of Sb_2S_3 and Sb_2Se_3 compounds. *Solid State Science* **14**, 1211–1220 (2012).
64. H. Koc, H. Ozisik, E. Deligoz, A. M. Mamedov, and E. Ozbay, Mechanical, electronic, and optical properties of Bi_2S_3 and Bi_2Se_3 compounds: first principle investigations. *Journal of Molecular Modeling.* **20**, 1–12 (2014).
65. L. Marton, Experiments on low-energy electron scattering and energy losess. *Rev Mod Phys.* **28**, 172–183 (1956).
66. O. V. Kovalev, Representations of the crystallographic space groups. *Irreducible representations induced representations and corepresentations*. Amsterdam: Gordon and Breach; 1965.